

QCD mesonic screening masses up to high temperatures

Mattia Dalla Brida,^a Leonardo Giusti,^{b,c} Tim Harris,^d Davide Laudicina^{b,c} and Michele Pepe^{c,*}

^a*Theoretical Physics Department, CERN,
1211 Geneva 23, Switzerland*

^b*Dipartimento di Fisica, Università di Milano-Bicocca,
Piazza della Scienza 3, I-20126 Milano, Italy*

^c*INFN, Sezione di Milano-Bicocca,
Piazza della Scienza 3, I-20126 Milano, Italy*

^d*School of Physics and Astronomy, University of Edinburgh,
Edinburgh EH9 3JZ, UK*

*E-mail: mattia.dalla.brida@cern.ch, Leonardo.Giusti@mib.infn.it,
tharris@ed.ac.uk, d.laudicina1@campus.unimib.it, pepe@mib.infn.it*

We discuss a strategy to study non-perturbatively QCD up to very high temperatures by Monte Carlo simulations on the lattice. It allows not only the thermodynamic properties of the theory but also other interesting thermal features to be investigated. As a first concrete application, we compute the flavour non-singlet mesonic screening masses and we present the results of Monte Carlo simulations at 12 temperatures covering the range from $T \sim 1$ GeV up to ~ 160 GeV in the theory with three massless quarks. On the one side, chiral symmetry restoration manifests itself in our results through the degeneracy of the vector and the axial vector channels and of the scalar and the pseudoscalar ones, and, on the other side, we observe a clear splitting between the vector and the pseudoscalar screening masses up to the highest investigated temperature. A comparison with the high-temperature effective theory shows that the known one-loop order in the perturbative expansion does not provide a satisfactory description of the non-perturbative data up to the highest temperature considered.

CERN-TH-2022-198

*41st International Conference on High Energy physics - ICHEP2022
6-13 July, 2022
Bologna, Italy*

*Speaker

1. Introduction

When QCD is studied at finite temperature T , a new energy scale influences the dynamics. In the low temperature regime, we have hadrons while when we consider very high temperatures we have a plasma of quarks and gluons that interact weakly. The understanding of high-temperature QCD is based on the idea that, when T is large, the dynamics is ruled by this energy scale and, due to asymptotic freedom, the gauge coupling becomes small. In those conditions, QCD behaves in practice as a 3-dimensional system. The gluon sector is given by a 3-dimensional Yang-Mills theory with gauge coupling g^2T involving the spatial components of the gauge field; the temporal component becomes an adjoint scalar field with a mass of the order of gT . The quarks pick up a mass proportional to T and are very heavy fields. Hence, taking this effective approach, we encounter three energy scales which, when the temperature is extremely high, are well separated, $g^2T/\pi \ll gT \ll \pi T$. In this setup the quarks are practically external sources and the main dynamics is related to the 3-dimensional Yang-Mills theory: thus, although the gauge coupling is weak, there are infrared non-perturbative effects that can be relevant [1–3].

First-principles non-perturbative information can be obtained studying QCD on the lattice however this is numerically challenging in the regime of high temperatures. On the one side, the state-of-the-art method to investigate QCD thermodynamics is based on the direct measurement of the trace anomaly of the Energy-Momentum tensor from which one can then obtain the other thermodynamics quantities. This method requires to consider always at the same time two different energy scales and the maximal temperature that has been reached is about 2 GeV. A second problem is related to the lack of knowledge of the parameters to use for the numerical simulations. For example, mesonic screening masses have been measured only up to about 1 GeV in the continuum limit [4–7]. Taking into account the inverse logarithmic behaviour of the gauge coupling with the temperature, the range of the explored temperatures is quite limited.

The first problem has been solved by studying thermodynamics in a moving reference frame [8–10]: this has the great advantage that one has to perform Monte Carlo simulations only at the physical temperature of interest. Using this approach, the thermodynamic features of the $SU(3)$ Yang-Mills theory have been measured very accurately up to high temperatures [11, 12] and work is in progress in QCD. For what concerns the lines of constant physics – namely, the parameter to consider in the Monte Carlo simulations – renormalizing the theory with a hadronic scheme is not a convenient choice since one has to consider a very fine lattice with a large size. A better choice is based on a finite volume scheme [13, 14] where, by performing successive steps in which the energy is doubled and the lattice spacing is halved, one can reach very high energies with a fine lattice spacing. Exploiting this strategy, one can investigate QCD at high temperatures and, as a first application, we have measured the mesonic screening masses [15].

2. Mesonic screening masses

Mesonic screening masses m_O characterize the long distance behaviour of mesonic two-point functions in the spatial direction

$$C_O(x_3) = \int dx_0 dx_1 dx_2 \langle O^a(x) O^a(0) \rangle \underset{x_3 \rightarrow \infty}{\sim} e^{-m_O x_3} \quad (1)$$

where $O^a(x) = \bar{\psi}(x) \Gamma T_a \psi(x)$, is a bilinear operator with T_a being the traceless generators of the flavour group and $\Gamma = \mathbb{1}, \gamma_5, \gamma_\mu, \gamma_\mu \gamma_5$ correspond to the scalar, pseudoscalar, vector and axial-vector screening masses respectively. They give information on the response of the system to the insertion of a mesonic operator as well as on the restoration of chiral symmetry. Screening masses are quite simple to measure numerically and we can also compare the non-perturbative results with the perturbative calculation that has been performed in the framework of the effective theory at one-loop order. For 3 flavours, it is given by [16]

$$m_O^{PT} = 2\pi T \left(1 + 0.032739961 g^2\right). \quad (2)$$

Notice that, at leading order, the mass is given by twice the mass of a static quark at finite temperature, πT , and that, at one-loop order, all the mesonic screening masses are degenerate.

3. The numerical study

We compute non-perturbatively the mesonic screening masses at 12 values of the temperature, T_0, \dots, T_{11} , approximately equally spaced in logarithmic scale from 160 GeV to 1 GeV. We regularize QCD on the lattice with 3 flavours of massless clover fermions; for the gauge sector we consider the Wilson action for T_0, \dots, T_8 and the tree-level improved Symanzik action for T_9, T_{10} and T_{11} .

Monte Carlo simulations are carried out on lattices with spatial size $L/a = 288$ and $LT > 20$ so to make finite size effects negligible. At each physical temperature, 3 or 4 different values of the lattice spacing a have been considered in order to extrapolate the results to the continuum limit; only for the temperature T_0 , the continuum limit has been obtained based on 2 values of the lattice spacing. We have run our numerical simulations considering shifted boundary conditions with shift $\xi = (1, 0, 0)$ since we have observed [12] that lattice artifacts are particularly small for that choice.

Effective masses are extracted from the expectation value of the two-point function C_O by

$$m_O(x_3) = \frac{1}{a} \operatorname{arccosh} \left[\frac{C_O(x_3 + a) + C_O(x_3 - a)}{2C_O(x_3)} \right] \quad (3)$$

and the screening mass m_O is obtained as the value at which the effective mass flattens when x_3 becomes large. In figure 1 we show the effective mass plots for the pseudoscalar and the vector screening masses at the temperature $T_3=33$ GeV obtained for a lattice with temporal extent $L_0/a = 6$. In both cases, we notice long plateaux that allow us to measure the screening masses with high accuracy and that are shown as bands in the plots.

At all the temperatures we have investigated, we observe a degeneracy between the scalar and the pseudoscalar screening masses as well as between the vector and the axial-vector ones: this is evidence for the restoration of chiral symmetry at high temperatures. More precisely, the $U_A(1)$ symmetry is anomalous also at finite temperature but the very strong suppression of the topological susceptibility taking place at high temperatures, makes the effects of the anomaly negligible w.r.t. the statistical uncertainty. For this reason we focus our discussion on the pseudoscalar, m_P , and on the vector, m_V , screening masses.

In order to ameliorate the approach to the continuum limit, we have introduced the following tree-level improved definition of the screening mass

$$m_O \longrightarrow m_O - \left[m_O^{\text{free}} - 2\pi T \right], \quad (4)$$

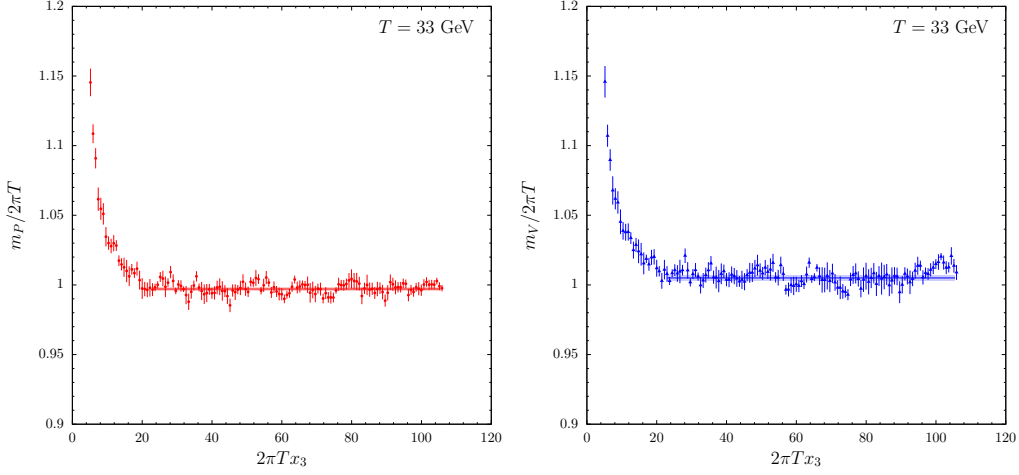


Figure 1: Plot of the effective masses, normalized to $2\pi T$, for the pseudoscalar (left) and vector (right) correlators at $T = 33$ GeV for $L_0/a = 6$. The two bands represent the estimate of the screening masses.

where m_O^{free} is the screening mass computed in the free lattice theory. In figure 2 we show the continuum limit extrapolations at the 12 temperatures we have considered. We notice that the $O(a)$ -improved fermion action, the improved definition of the screening mass and the use of shifted boundary conditions with shift vector $\xi = (1, 0, 0)$ make the discretization effects very mild and we attain a final accuracy in the continuum limit of a few permille.

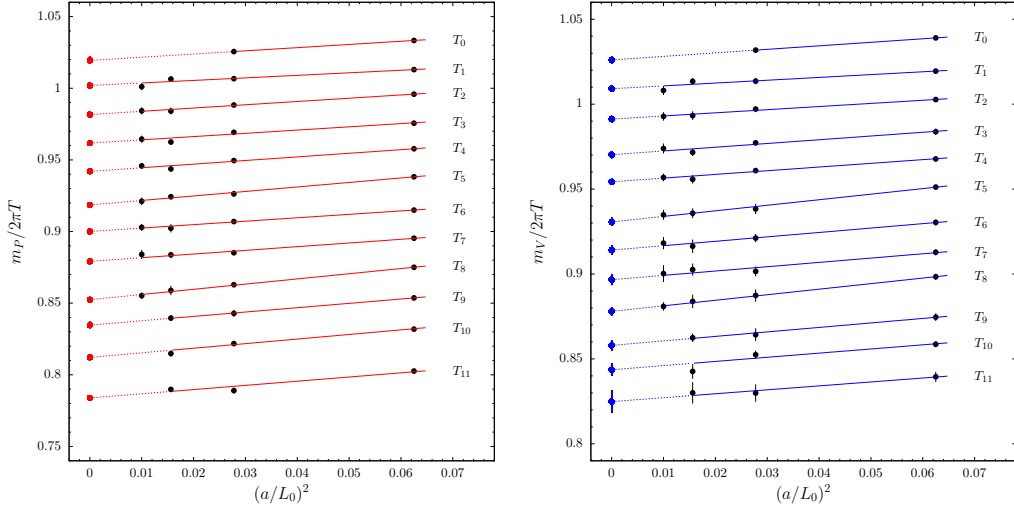


Figure 2: Continuum limit extrapolations for the tree-level improved pseudoscalar (left panel) and vector (right panel) screening masses. Each temperature is analyzed independently from the others. Data corresponding to T_i ($i = 0, \dots, 11$) are shifted downward by $0.02 \times i$ for better readability.

In figure 3 we present the temperature dependence of the pseudoscalar and of the vector screening masses: the data are those resulting from the continuum limit extrapolations of figure 2.

The straight line represents the one-loop perturbative result given by eq. (2). The dependence on the temperature is expressed in terms of the function $\hat{g}^2(T)$ defined as

$$\frac{1}{\hat{g}^2(T)} \equiv \frac{9}{8\pi^2} \ln \frac{2\pi T}{\Lambda_{\overline{\text{MS}}}} + \frac{4}{9\pi^2} \ln \left(2 \ln \frac{2\pi T}{\Lambda_{\overline{\text{MS}}}} \right), \quad (5)$$

where $\Lambda_{\overline{\text{MS}}} = 341$ MeV is taken from Ref. [17]. Although it corresponds to the two-loop $\overline{\text{MS}}$ definition of the strong coupling constant at the scale $\mu = 2\pi T$, for our purposes it is just a function of the temperature T , suggested by the effective theory analysis, that we use to analyze our results: the crucial point is the leading logarithmic dependence on T . The blue and the red bands are fits of the numerical data up to order $\hat{g}^4(T)$. We refer the reader to [15] for a detailed discussion of the data analysis.

4. Conclusion

In these proceedings we have presented a strategy to investigate QCD up to very high temperatures. On the one side, we consider shifted boundary conditions that represent an effective framework to investigate thermodynamics (and for $\xi = (1, 0, 0)$ give, in general, very small lattice artifacts) and, on the other side, we match T with the energy scale of the running coupling defined with the step-scaling technique in order to determine the parameters for the Monte Carlo simulations. We show results for mesonic screening masses at temperatures ranging from 1 GeV to 160 GeV and we compare our non-perturbative results with the one-loop perturbative computation: contrary to the expectation coming from the latter, we observe a splitting between pseudoscalar and vector screening masses for all the investigated temperatures. We find also evidence for a degeneracy between the scalar and the pseudoscalar masses as well as between the vector and the axial-vector ones.

Acknowledgements We acknowledge PRACE for awarding us access to the HPC system MareNostrum4 at the Barcelona Supercomputing Center (Proposals n. 2018194651 and 2021240051). We also thank CINECA for providing us with computer-time on Marconi (CINECA- INFN, CINECA-Bicocca agreements, ISCR A B projects HP10BF2OQT and HP10B1TWRR).

References

- [1] P. H. Ginsparg, *First Order and Second Order Phase Transitions in Gauge Theories at Finite Temperature*, *Nucl. Phys. B* **170** (1980) 388–408.
- [2] T. Appelquist and R. D. Pisarski, *High-Temperature Yang-Mills Theories and Three-Dimensional Quantum Chromodynamics*, *Phys. Rev. D* **23** (1981) 2305.

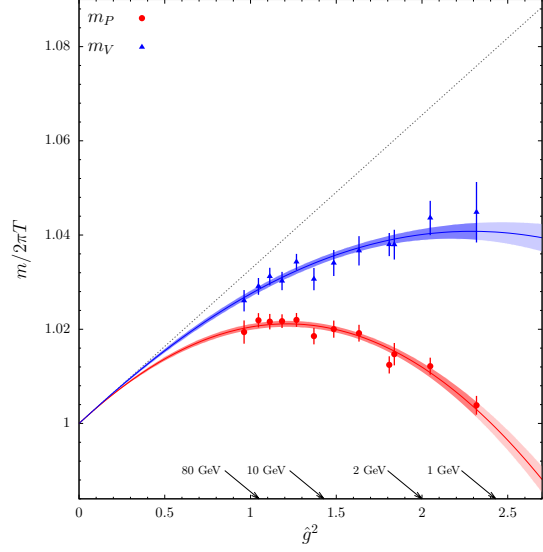


Figure 3: Pseudoscalar (red) and vector (blue) screening masses versus \hat{g}^2 . The bands represent the best fits up to order \hat{g}^4 , while the dashed line is eq. (2).

- [3] E. Braaten and A. Nieto, *Free energy of QCD at high temperature*, *Phys. Rev. D* **53** (1996) 3421–3437, [[hep-ph/9510408](#)].
- [4] M. Cheng et al., *Meson screening masses from lattice QCD with two light and the strange quark*, *Eur. Phys. J. C* **71** (2011) 1564, [[arXiv:1010.1216](#)].
- [5] B. B. Brandt, A. Francis, M. Laine, and H. B. Meyer, *A relation between screening masses and real-time rates*, *JHEP* **05** (2014) 117, [[arXiv:1404.2404](#)].
- [6] A. Bazavov et al., *Meson screening masses in (2+1)-flavor QCD*, *Phys. Rev. D* **100** (2019), no. 9 094510, [[arXiv:1908.09552](#)].
- [7] B. B. Brandt, O. Philipsen, M. Cè, A. Francis, T. Harris, H. B. Meyer, and H. Wittig, *Testing the strength of the $U_A(1)$ anomaly at the chiral phase transition in two-flavour QCD*, *PoS CD2018* (2019) 055, [[arXiv:1904.02384](#)].
- [8] L. Giusti and H. B. Meyer, *Thermodynamic potentials from shifted boundary conditions: the scalar-field theory case*, *JHEP* **11** (2011) 087, [[arXiv:1110.3136](#)].
- [9] L. Giusti and H. B. Meyer, *Thermal momentum distribution from path integrals with shifted boundary conditions*, *Phys. Rev. Lett.* **106** (2011) 131601, [[arXiv:1011.2727](#)].
- [10] L. Giusti and H. B. Meyer, *Implications of Poincare symmetry for thermal field theories in finite-volume*, *JHEP* **01** (2013) 140, [[arXiv:1211.6669](#)].
- [11] L. Giusti and M. Pepe, *Equation of state of a relativistic theory from a moving frame*, *Phys. Rev. Lett.* **113** (2014) 031601, [[arXiv:1403.0360](#)].
- [12] L. Giusti and M. Pepe, *Equation of state of the $SU(3)$ Yang–Mills theory: A precise determination from a moving frame*, *Phys. Lett.* **B769** (2017) 385–390, [[arXiv:1612.00265](#)].
- [13] M. Lüscher, P. Weisz, and U. Wolff, *A numerical method to compute the running coupling in asymptotically free theories*, *Nucl. Phys.* **B359** (1991) 221–243.
- [14] K. Jansen et al., *Non-perturbative renormalization of lattice QCD at all scales*, *Phys. Lett.* **B372** (1996) 275–282, [[hep-lat/9512009](#)].
- [15] M. Dalla Brida, L. Giusti, T. Harris, D. Laudicina, and M. Pepe, *Non-perturbative thermal QCD at all temperatures: the case of mesonic screening masses*, *JHEP* **04** (2022) 034, [[arXiv:2112.05427](#)].
- [16] M. Laine and M. Vepsalainen, *Mesonic correlation lengths in high temperature QCD*, *JHEP* **02** (2004) 004, [[hep-ph/0311268](#)].
- [17] ALPHA Collaboration, M. Bruno, M. Dalla Brida, P. Fritzsche, T. Korzec, A. Ramos, S. Schaefer, H. Simma, S. Sint, and R. Sommer, *QCD Coupling from a Nonperturbative Determination of the Three-Flavor Λ Parameter*, *Phys. Rev. Lett.* **119** (2017), no. 10 102001, [[arXiv:1706.03821](#)].